



Tunable-focus microlens arrays using nanosized polymer-dispersed liquid crystal droplets

Hongwen Ren, Yun-Hsing Fan, Yi-Hsin Lin, Shin-Tson Wu *

College of Optics and Photonics, University of Central Florida, 4000 Central Florida Blvd., Orlando, FL 32816, USA

Received 18 August 2004; received in revised form 3 November 2004; accepted 8 November 2004

Abstract

A microlens array made of polymer/nanosized polymer-dispersed liquid crystal (nano-PDLC) is demonstrated. The polymer was first patterned into microlens array cavities on a planar substrate and the molded polymer cavities were filled with nano-PDLC material. The nano-PDLC-based microlens is optically transparent. The focal length of the microlens is electrically tunable and the response time is about 200 μ s during focus change. Such an electrically tunable-focus lens is a broadband device and its performance is independent of light polarization. A tradeoff is the high operating voltage.

© 2004 Elsevier B.V. All rights reserved.

Keywords: Liquid crystal microlens; Nanosized polymer-dispersed liquid crystal; Tunable focal length

1. Introduction

Electrically tunable-focus liquid crystal (LC) lenses have been studied extensively in recent years and various approaches have been proposed [1–12]. Among them, the LC based microlens array is promising for optoelectronics, integrated optics, information processing, and optical communications. To tune the focal length by an external electric field, the refractive index profile from the lens

edges to the center should be changeable. Most of the LC lenses demonstrated so far use homogeneous molecular alignment because of its pure phase modulation. However, the homogeneous cell is sensitive to the input light polarization, i.e., a linearly polarized light or an unpolarized light with a sheet polarizer has to be used. The use of a sheet polarizer reduces the optical efficiency by at least 50%. Moreover, the birefringence effect causes a large aberration for the oblique angle incident light and chromatic dispersion due to the wavelength-dependent LC birefringence [13].

Another common issue of the conventional LC lenses is the slow response time during focus

* Corresponding author. Tel.: +1 4078234763; fax: +1 4078236880.

E-mail address: swu@mail.ucf.edu (S.-T. Wu).

change [14]. To improve response time, polymer stabilized technique has been investigated [11]. Due to the anchoring effect of polymer networks, the response time can be improved significantly, depending upon the polymer concentration. Although a higher polymer concentration leads to a faster response time, the associated light scattering is increased.

Recently, we proposed a lamination method for fabricating microlens arrays [12]. This technique is quite simple and the formed LC lens curvature is spherical. However, the LC molecules are in homogeneous alignment so that the device is polarization dependent. The response time is around 30 ms.

To realize a polarization independent LC lens with fast response time, in this paper, we report a two-dimensional (2D) microlens array using nanosized polymer-dispersed liquid crystal (nano-PDLC) droplets. Because of the small droplet sizes, the nano-PDLC approach exhibits three major advantages: scattering-free, polarization-independent, and fast response time. Moreover, the LC droplets are randomly oriented in the polymer matrix, the aberration from oblique angles is greatly reduced. The major shortcoming is the increased operating voltage.

2. Device fabrication

During device fabrication, the polymer is first molded to form plano-concave microlens arrays. The cavities of the lenses are filled with nano-PDLC material. The lens materials used in this study are UV-curable prepolymer (NOA65; its refractive index $n_p = 1.524$) and Merck nematic LC E48 ($n_o = 1.523$, $\Delta n = 0.231$). The LC host and NOA65 were mixed at 35:65 wt% ratios. To fabricate the 2D microlens arrays, we first coated the pure prepolymer NOA65 onto an indium-tin-oxide (ITO) glass substrate. Next, we used a glass plano-convex microlens arrays as a stamper to laminate the coated prepolymer NOA65. The thickness and diameter of each microlens is 45 μm and 450 μm , respectively. The laminated NOA65 was exposed to UV light. After UV exposure, the stamper was peeled off. At this stage, the

solidified polymer surface exhibits concave microlens patterns on the ITO-glass substrate. The LC/NOA65 mixture was injected into the cavities of the stamped polymer layer and then sealed with a top ITO-glass substrate. Because of the high UV sensitivity and high concentration in the LC mixture, NOA65 can be cured rapidly using a relatively low intensity ($I \sim 15 \text{ mW/cm}^2$). The curing time is ~ 30 min for obtaining saturated phase separation between NOA65 and LC-E48. The curing temperature was kept at $\sim 50^\circ\text{C}$ in order to ensure that the phase separation is induced by UV light, not influenced by the temperature variation.

3. Operation principle

Figs. 1(a) and (b) depict the side view of the nano-PDLC lens in the voltage-off and voltage-on states, respectively. This plano-lens can be viewed as a combination of a plano-convex nano-PDLC lens and a molded plano-concave polymer lens. In our studies, we used the same polymer for the molded lens and nano-PDLC. The ordinary refractive index of the LC material matches well with that of the polymer matrix, i.e., $n_o \sim n_p$. Thus, the spherical profile is contributed by the lens-shaped LC droplets. In the convex PDLC lens region, as depicted in Fig. 1(a), the LC droplets are uniformly dispersed in polymer matrix. When the electric field is absent, the refractive index is the same at any direction because the LC droplets are randomly oriented. The effective refractive index (n_{eff}) of the nano-PDLC is larger than n_p . The focal length of the LC microlens

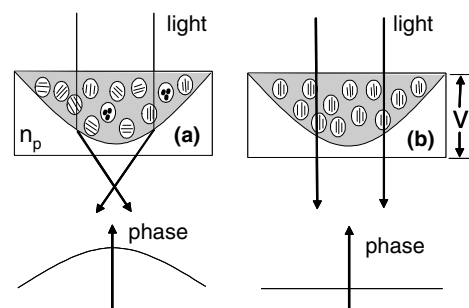


Fig. 1. Side view of the nano-PDLC lens in the: (a) voltage-off, and (b) voltage-on states.

can be evaluated using Fresnel's approximation [15] as

$$f = \frac{r^2}{2d\delta n}. \quad (1)$$

In Eq. (1), r is the radius of the lens, d is the cell gap, and δn is the refractive index difference between the lens center and border. In the voltage-off state, δn is the largest, i.e., the gradient of the phase profile across the lens diameter is the sharpest, so that the focal length f is the shortest, as depicted in Fig. 1(a). When the applied voltage is sufficiently high, the LC molecules are reoriented along the electric field direction. The effective refractive index in the plane perpendicular to the electric field is decreased. This decrease in refractive index will reduce the phase profile gradient, as shown in Fig. 1(b). As a result, the focal length increases. In a very high voltage regime where $n_{\text{eff}} \sim n_p$, the focusing effect disappears and the focal length turns to infinity when the incident light is perpendicular to the lens surface. Because the LC droplet is smaller than the visible wavelength, the lens is highly transparent; it does not scatter

light. Moreover, the microlens is polarization independent and its response speed is fast.

4. Experimental setup

Fig. 2 shows the experimental setup for measuring the 2D focused spot patterns and the focal length of the microlens arrays. The sample was mounted on a linear metric stage. A collimated unpolarized He–Ne laser beam ($\lambda = 633 \text{ nm}$) was used to illuminate the sample. The transmitted light was collected by an imaging lens (L_1) and detected by a CCD camera (SBIG model ST-2000XM). The detected data were analyzed by a computer.

5. Results and discussions

The microlens array we fabricated is slight bluish which implies that the formed LC droplet size is comparable to a blue wavelength ($\lambda \sim 400 \text{ nm}$). However, the entire sample is highly transparent at the He–Ne laser wavelength ($\lambda = 633 \text{ nm}$) which we used for measuring optical properties. To inspect the quality of the formed microlens profile, we placed the microlens sample on a polarized optical microscope; no voltage was applied to the cell. Three photos were taken, as shown in Fig. 3. Fig. 3(a) shows the textures of the sample without polarizer. Clearly, very regular and uniform circular convex lenses with 0.45-mm diameter are formed. Fig. 3(b) shows the microlens textures under crossed polarizers. Some wide concentric rings

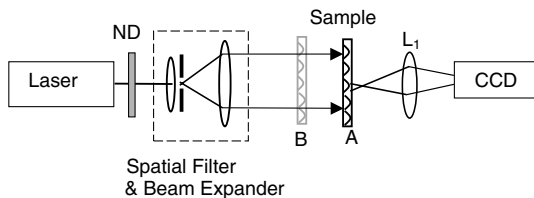


Fig. 2. Experimental setup for characterizing the nano-PDLC microlens arrays. ND, neutral density filter, and L_1 , imaging lens.

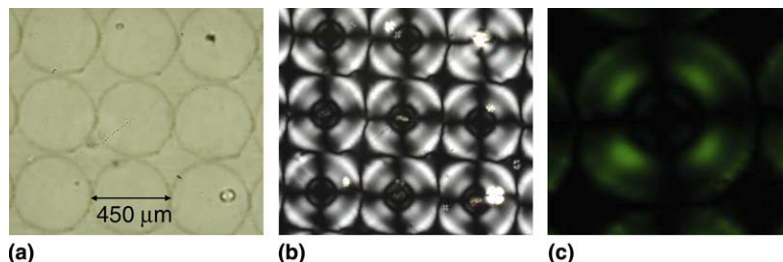


Fig. 3. Photos of a convex microlens array observed using a polarized optical microscope: (a) without polarizer, (b) crossed polarizers and (c) same as (b) but with a green filter.

are clearly visible although no color filter was added to the microscope white light source. The black cross observed in each microlens indicates that the nematic LC domains in polymer matrix have an isotropic director distribution. When the sample is rotated gradually, the position of the black cross does not change. The wide circular ring originates from the gradient phase retardation. Between the adjacent rings, the phase difference is 2π . To estimate the total phase retardation at $\lambda = 633$ nm, we first use a green color filter ($\lambda \sim 540$ nm; sensitive to eye) to observe the fringes of a microlens, and then convert the measured phase retardation to $\lambda = 633$ nm. As shown in Fig. 3(c), the total phase difference from the center to the borders is $\sim 3\pi$ at $\lambda \sim 540$ nm which is equivalent to $\sim 2.5\pi$ at $\lambda = 633$ nm.

To measure the focal length of the microlens arrays at voltage-off state, we placed the sample at a position A, as shown in Fig. 2. By adjusting the distance of imaging lens L_1 , a clear image of the microlens surface is displayed on the CCD camera screen, as shown in Fig. 4(a). The measured average intensity of each microlens reaches ~ 300 arbitrary units. If the microlens array is moved toward the laser source, e.g., position B, we obtain the sharpest focal points as shown in Fig. 4(b). The converging effect implies that this is a positive lens. The intensity profiles of the focal spots were also measured. At position B, the peak intensity is the strongest ($>22,000$ arbitrary units). The distance from A to B is 3.3 cm; this is the focal length of the microlens.

The voltage-dependent focal length of the microlens is also investigated and the results are

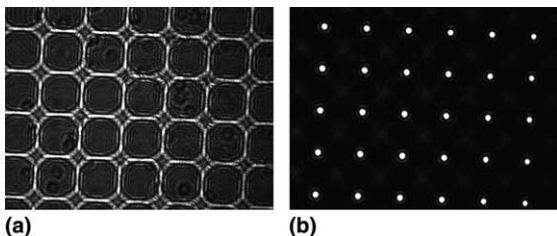


Fig. 4. (a) An image of the microlens surface recorded by the CCD camera at position A. (b) Arrays of light spots at position B.

plotted in Fig. 5. At a given voltage, all the focal spots of the LC microlens arrays appear in the same focal plane due to the same lens size and the same nano-PDLC structure. At $V = 0$ the focal length is ~ 3.3 cm. When the applied voltage exceeds $V = 100$ V_{rms}, the focal length gradually increases. In principle, if the applied voltage $V \rightarrow \infty$, all the LC directors inside the droplets are reoriented by the electric field so that the focusing behavior should disappear, i.e., $f \rightarrow \infty$. However, electric breakdown may take place before this extreme condition is realized. The error bars shown in Fig. 5 result from the uncertainty in determining the beam waist.

From Eq. (1), we could estimate the refractive index change δn of the nano-PDLC. In our design, $r = 225$ μm , $d \sim 45$ μm , and $2d\delta n \sim 2.5\lambda$ (from Fig. 3(b)). For the He–Ne laser beam we used ($\lambda = 633$ nm), we find $f \sim 3.3$ cm and $\delta n \sim 0.018$. This result is slightly smaller than the ideal refractive index change of a PDLC, which is $c\Delta n/3$; Δn being the LC birefringence and c , the LC concentration. For the nano-PDLC we prepared, $c \sim 35\%$ and $\Delta n \sim 0.23$. As a result, the theoretical refractive index change should be 0.027. The observed δn is somewhat smaller than the theoretical value. This is because a portion of the LC material is dissolved in the polymer matrix and cannot be reoriented even in the high voltage regime. Thus, the effective LC concentration is smaller than the theoretical one.

From Eq. (1), three factors affect the focal length: lens radius, LC cell gap, and refractive index difference. For a given lens radius and cell

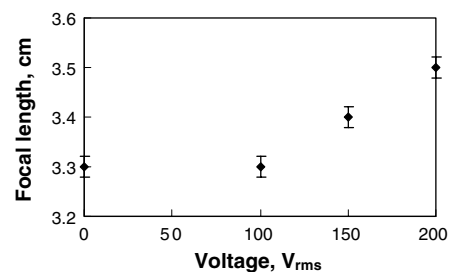


Fig. 5. Voltage-dependent focal length of the nano-PDLC microlens array. LC cell gap $d = 45$ μm , the microlens diameter $D = 450$ μm , and $\lambda = 633$ nm.

gap, we could employ a higher birefringence LC to achieve a shorter focal length. To overcome the high voltage problem of the nano-PDLC lens, we could use a thinner cell filled with a high birefringence and high $\Delta\epsilon$ LC [16]. Adding a small amount of surfactant to the nano-PDLC film is helpful for lowering the operating voltage [17].

Response time is a very important factor for a tunable lens, especially during focus change. To measure the response time of the microlens, a CCD camera as shown in Fig. 2 was replaced by a photodetector. A pinhole was placed right before the photodetector. At $V = 0$, the pinhole aperture was kept small so that the cone-shaped beam can pass through the aperture without any loss. The intensity of the beam is I_0 . As voltage is applied to the microlens, the focal length of the microlens becomes longer. Under such a circumstance, the laser beam diameter is larger than the pinhole aperture and a portion of the beam is truncated by the pinhole. The intensity of the transmitted beam is reduced to I . The response times corresponding to the transmittance change from I_0 to I and from I to I_0 were measured using a computer controlled LabVIEW data acquisition system. By applying a gated square wave of 1s width and 200 V_{rms} (1 kHz) pulse amplitude to the sample, the response times (recorded from oscilloscope traces) from the focused to less focused (τ_1) and from less focused to focused (τ_2) states were measured. Results are shown in Fig. 6. From Fig. 6, τ_1 is found to be $\sim 250 \mu\text{s}$ and $\tau_2 \sim 150 \mu\text{s}$, respectively. Based on these results, the LC droplet diameter is estimated to be around 300 nm, which is indeed shorter than the blue wavelength.

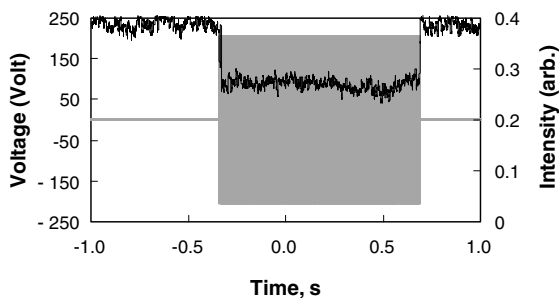


Fig. 6. The measured response time of the nano-PDLC microlens. $\tau_1 \sim 250 \mu\text{s}$ and $\tau_2 \sim 150 \mu\text{s}$.

In comparison with other tunable microlens technologies using pure nematic LC, the magnitude of the focal length change of the nano-PDLC microlens is relatively small. This is because the LC concentration is only 35% and the droplets are randomly oriented. However, the nano-PDLC microlens array has several advantages, such as simple fabrication process, ideal concave spherical shape, independent of polarization, and fast (sub-millisecond) response time. The microlens array is highly transparent and the optical efficiency of each microlens can reach 100% for an unpolarized light. Unlike polymer network LC lens, the nano-PDLC lens is very stable even it is operated at a high voltage. Potential applications of the demonstrated nano-PDLC microlens can be found in optics communications and information processing.

6. Conclusion

We have demonstrated a simple method for fabricating tunable-focus nano-PDLC microlens arrays. Such a microlens array is polarization independent and has sub-millisecond response time. Without voltage, the microlens has an inherent focal length ~ 3.3 cm. As the applied voltage exceeds a threshold, the LC reorientation occurs and the focal length of the microlens gradually increases. Using this method, both positive and negative microlens can be fabricated fairly easily.

Acknowledgment

This work is supported by DARPA BOSS program under Contract No. W911NF04C0048.

References

- [1] S. Sato, Jpn. J. Appl. Phys. 18 (1979) 1679.
- [2] T. Nose, S. Sato, Liq. Cryst. 5 (1989) 1425.
- [3] J.S. Patel, K. Rastani, Opt. Lett. 16 (1991) 532.
- [4] N.A. Riza, M.C. DeJule, Opt. Lett. 19 (1994) 1013.
- [5] A.F. Naumov, G.D. Love, M.Yu. Loktev, F.L. Vladimirov, Opt. Express 4 (1999) 344.
- [6] W. Klaus, M. Ide, Y. Hayano, S. Morokawa, Y. Arimoto, Proc. SPIE 3635 (1999) 66.

- [7] L.G. Commander, S.E. Day, D.R. Selviah, *Opt. Commun.* 177 (2000) 157.
- [8] Y. Choi, J.H. Park, J.H. Kim, S.D. Lee, *Opt. Mater.* 21 (2002) 643.
- [9] V. Presnyakov, K. Asatryan, T. Galstian, A. Tork, *Opt. Express* 26 (2002) 865.
- [10] H.S. Ji, J.H. Kim, S. Kumar, *Opt. Lett.* 28 (2003) 1147.
- [11] H. Ren, Y.H. Fan, S. Gauza, S.T. Wu, *Opt. Commun.* 230 (2004) 267.
- [12] H. Ren, Y.H. Fan, S.T. Wu, *Opt. Lett.* 29 (2004) 1608.
- [13] S.T. Wu, *Phys. Rev. A* 33 (1986) 1270.
- [14] H. Ren, Y.H. Fan, S. Gauza, S.T. Wu, *Appl. Phys. Lett.* 84 (2004) 4789.
- [15] J.W. Goodman, *Introduction to Fourier Optics*, McGraw-Hill, New York, 1968.
- [16] S.T. Wu, D.K. Yang, *Reflective Liquid Crystal Displays*, Wiley, New York, 2001.
- [17] V.P. Tondiglia, L.V. Natarajan, R.L. Sutherland, T.J. Bunning, W.W. Adams, *Opt. Lett.* 20 (1995) 1325.